

Measurement of the W^+W^- Production Cross Section in $\bar{p}p$ Collisions at $\sqrt{s}=1.96$ TeV using Dilepton Events

D. Acosta,¹⁶ J. Adelman,¹² T. Affolder,⁹ T. Akimoto,⁵⁴ M. G. Albrow,¹⁵ D. Ambrose,⁴³ S. Amerio,⁴² D. Amidei,³³ A. Anastassov,⁵⁰ K. Anikeev,¹⁵ A. Annovi,⁴⁴ J. Antos,¹ M. Aoki,⁵⁴ G. Apollinari,¹⁵ T. Arisawa,⁵⁶ J.-F. Arguin,³² A. Artikov,¹³ W. Ashmanskas,¹⁵ A. Attal,⁷ F. Azfar,⁴¹ P. Azzi-Bacchetta,⁴² N. Bacchetta,⁴² H. Bachacou,²⁸ W. Badgett,¹⁵ A. Barbaro-Galtieri,²⁸ G. J. Barker,²⁵ V. E. Barnes,⁴⁶ B. A. Barnett,²⁴ S. Baroiant,⁶ M. Barone,¹⁷ G. Bauer,³¹ F. Bedeschi,⁴⁴ S. Behari,²⁴ S. Belforte,⁵³ G. Bellettini,⁴⁴ J. Bellinger,⁵⁸ E. Ben-Haim,¹⁵ D. Benjamin,¹⁴ A. Beretvas,¹⁵ A. Bhatti,⁴⁸ M. Binkley,¹⁵ D. Bisello,⁴² M. Bishai,¹⁵ R. E. Blair,² C. Blocker,⁵ K. Bloom,³³ B. Blumenfeld,²⁴ A. Bocci,⁴⁸ A. Bodek,⁴⁷ G. Bolla,⁴⁶ A. Bolshov,³¹ P. S. L. Booth,²⁹ D. Bortoletto,⁴⁶ J. Boudreau,⁴⁵ S. Bourov,¹⁵ B. Brau,⁹ C. Bromberg,³⁴ E. Brubaker,¹² J. Budagov,¹³ H. S. Budd,⁴⁷ K. Burkett,¹⁵ G. Busetto,⁴² P. Bussey,¹⁹ K. L. Byrum,² S. Cabrera,¹⁴ M. Campanelli,¹⁸ M. Campbell,³³ F. Canelli,⁷ A. Canepa,⁴⁶ M. Casarsa,⁵³ D. Carlsmith,⁵⁸ S. Carron,¹⁴ R. Carosi,⁴⁴ M. Cavalli-Sforza,³ A. Castro,⁴ P. Catastini,⁴⁴ D. Cauz,⁵³ A. Cerri,²⁸ L. Cerrito,²³ J. Chapman,³³ C. Chen,⁴³ Y. C. Chen,¹ M. Chertok,⁶ G. Chiarelli,⁴⁴ G. Chlachidze,¹³ F. Chlebana,¹⁵ I. Cho,²⁷ K. Cho,²⁷ D. Chokheli,¹³ J. P. Chou,²⁰ M. L. Chu,¹ S. Chuang,⁵⁸ J. Y. Chung,³⁸ W.-H. Chung,⁵⁸ Y. S. Chung,⁴⁷ C. I. Ciobanu,²³ M. A. Ciocci,⁴⁴ A. G. Clark,¹⁸ D. Clark,⁵ M. Coca,⁴⁷ A. Connolly,²⁸ M. Convery,⁴⁸ J. Conway,⁶ B. Cooper,³⁰ M. Cordelli,¹⁷ G. Cortiana,⁴² J. Cranshaw,⁵² J. Cuevas,¹⁰ R. Culbertson,¹⁵ C. Currat,²⁸ D. Cyr,⁵⁸ D. Dagenhart,⁵ S. Da Ronco,⁴² S. D'Auria,¹⁹ P. de Barbaro,⁴⁷ S. De Cecco,⁴⁹ G. De Lentdecker,⁴⁷ S. Dell'Agnello,¹⁷ M. Dell'Orso,⁴⁴ S. Demers,⁴⁷ L. Demortier,⁴⁸ J. Deng,¹⁴ M. Deninno,⁴ D. De Pedis,⁴⁹ P. F. Derwent,¹⁵ C. Dionisi,⁴⁹ J. R. Dittmann,¹⁵ C. Dörr,²⁵ P. Doksus,²³ A. Dominguez,²⁸ S. Donati,⁴⁴ M. Donega,¹⁸ J. Donini,⁴² M. D'Onofrio,¹⁸ T. Dorigo,⁴² V. Drollinger,³⁶ K. Ebina,⁵⁶ N. Eddy,²³ J. Efron,³⁸ J. Ehlers,¹⁸ R. Ely,²⁸ R. Erbacher,⁶ M. Erdmann,²⁵ D. Errede,²³ S. Errede,²³ R. Eusebi,⁴⁷ H.-C. Fang,²⁸ S. Farrington,²⁹ I. Fedorko,⁴⁴ W. T. Fedorko,¹² R. G. Feild,⁵⁹ M. Feindt,²⁵ J. P. Fernandez,⁴⁶ C. Ferretti,³³ R. D. Field,¹⁶ G. Flanagan,³⁴ B. Flaughner,¹⁵ L. R. Flores-Castillo,⁴⁵ A. Foland,²⁰ S. Forrester,⁶ G. W. Foster,¹⁵ M. Franklin,²⁰ J. C. Freeman,²⁸ Y. Fujii,²⁶ I. Furic,¹² A. Gajjar,²⁹ A. Gallas,³⁷ J. Galyardt,¹¹ M. Gallinaro,⁴⁸ M. Garcia-Sciveres,²⁸ A. F. Garfinkel,⁴⁶ C. Gay,⁵⁹ H. Gerberich,¹⁴ D. W. Gerdes,³³ E. Gerchtein,¹¹ S. Giagu,⁴⁹ P. Giannetti,⁴⁴ A. Gibson,²⁸ K. Gibson,¹¹ C. Ginsburg,⁵⁸ K. Giolo,⁴⁶ M. Giordani,⁵³ M. Giunta,⁴⁴ G. Giurgiu,¹¹ V. Glagolev,¹³ D. Glenzinski,¹⁵ M. Gold,³⁶ N. Goldschmidt,³³ D. Goldstein,⁷ J. Goldstein,⁴¹ G. Gomez,¹⁰ G. Gomez-Ceballos,¹⁰ M. Goncharov,⁵¹ O. González,⁴⁶ I. Gorelov,³⁶ A. T. Goshaw,¹⁴ Y. Gotra,⁴⁵ K. Goulianos,⁴⁸ A. Gresele,⁴ M. Griffiths,²⁹ C. Grosso-Pilcher,¹² U. Grundler,²³ M. Guenther,⁴⁶ J. Guimaraes da Costa,²⁰ C. Haber,²⁸ K. Hahn,⁴³ S. R. Hahn,¹⁵ E. Halkiadakis,⁴⁷ A. Hamilton,³² B.-Y. Han,⁴⁷ R. Handler,⁵⁸ F. Happacher,¹⁷ K. Hara,⁵⁴ M. Hare,⁵⁵ R. F. Harr,⁵⁷ R. M. Harris,¹⁵ F. Hartmann,²⁵ K. Hatakeyama,⁴⁸ J. Hauser,⁷ C. Hays,¹⁴ H. Hayward,²⁹ E. Heider,⁵⁵ B. Heinemann,²⁹ J. Heinrich,⁴³ M. Hennecke,²⁵ M. Herndon,²⁴ C. Hill,⁹ D. Hirschbuehl,²⁵ A. Hocker,⁴⁷ K. D. Hoffman,¹² A. Holloway,²⁰ S. Hou,¹ M. A. Houlden,²⁹ B. T. Huffman,⁴¹ Y. Huang,¹⁴ R. E. Hughes,³⁸ J. Huston,³⁴ K. Ikado,⁵⁶ J. Incandela,⁹ G. Introzzi,⁴⁴ M. Iori,⁴⁹ Y. Ishizawa,⁵⁴ C. Issever,⁹ A. Ivanov,⁴⁷ Y. Iwata,²² B. Iyutin,³¹ E. James,¹⁵ D. Jang,⁵⁰ J. Jarrell,³⁶ D. Jeans,⁴⁹ H. Jensen,¹⁵ E. J. Jeon,²⁷ M. Jones,⁴⁶ K. K. Joo,²⁷ S. Y. Jun,¹¹ T. Junk,²³ T. Kamon,⁵¹ J. Kang,³³ M. Karagoz Unel,³⁷ P. E. Karchin,⁵⁷ S. Kartal,¹⁵ Y. Kato,⁴⁰ Y. Kemp,²⁵ R. Kephart,¹⁵ U. Kerzel,²⁵ V. Khotilovich,⁵¹ B. Kilminster,³⁸ D. H. Kim,²⁷ H. S. Kim,²³ J. E. Kim,²⁷ M. J. Kim,¹¹ M. S. Kim,²⁷ S. B. Kim,²⁷ S. H. Kim,⁵⁴ T. H. Kim,³¹ Y. K. Kim,¹² M. Kirby,¹⁴ L. Kirsch,⁵ S. Klimentenko,¹⁶ B. Knuteson,³¹ B. R. Ko,¹⁴ H. Kobayashi,⁵⁴ P. Koehn,³⁸ D. J. Kong,²⁷ K. Kondo,⁵⁶ J. Konigsberg,¹⁶ K. Kordas,³² A. Korn,³¹ A. Korytov,¹⁶ K. Kotelnikov,³⁵ A. V. Kotwal,¹⁴ A. Kovalev,⁴³ J. Kraus,²³ I. Kravchenko,³¹ A. Kreymer,¹⁵ J. Kroll,⁴³ M. Kruse,¹⁴ V. Krutelyov,⁵¹ S. E. Kuhlmann,² S. Kwang,¹² A. T. Laasanen,⁴⁶ S. Lai,³² S. Lami,⁴⁴ S. Lammel,¹⁵ J. Lancaster,¹⁴ M. Lancaster,³⁰ R. Lander,⁶ K. Lannon,³⁸ A. Lath,⁵⁰ G. Latino,³⁶ R. Lauhakangas,²¹ I. Lazzizzera,⁴² Y. Le,²⁴ C. Lecci,²⁵ T. LeCompte,² J. Lee,²⁷ J. Lee,⁴⁷ S. W. Lee,⁵¹ R. Lefèvre,³ N. Leonardo,³¹ S. Leone,⁴⁴ S. Levy,¹² J. D. Lewis,¹⁵ K. Li,⁵⁹ C. Lin,⁵⁹ C. S. Lin,¹⁵ M. Lindgren,¹⁵ T. M. Liss,²³ A. Lister,¹⁸ D. O. Litvintsev,¹⁵ T. Liu,¹⁵ Y. Liu,¹⁸ N. S. Lockyer,⁴³ A. Loginov,³⁵ M. Loretì,⁴² P. Loverre,⁴⁹ R.-S. Lu,¹ D. Lucchesi,⁴² P. Lujan,²⁸ P. Lukens,¹⁵ G. Lungu,¹⁶ L. Lyons,⁴¹ J. Lys,²⁸ R. Lysak,¹ D. MacQueen,³² R. Madrak,¹⁵ K. Maeshima,¹⁵ P. Maksimovic,²⁴ L. Malferrari,⁴ G. Manca,²⁹ R. Marginean,³⁸ C. Marino,²³ A. Martin,²⁴ M. Martin,⁵⁹ V. Martin,³⁷ M. Martínez,³ T. Maruyama,⁵⁴ H. Matsunaga,⁵⁴ M. Mattson,⁵⁷ P. Mazzanti,⁴ K. S. McFarland,⁴⁷ D. McGivern,³⁰ P. M. McIntyre,⁵¹ P. McNamara,⁵⁰ R. McNulty,²⁹ A. Mehta,²⁹ S. Menzemer,³¹ A. Menzione,⁴⁴ P. Merkel,¹⁵ C. Mesropian,⁴⁸ A. Messina,⁴⁹ T. Miao,¹⁵ N. Miladinovic,⁵ L. Miller,²⁰ R. Miller,³⁴ J. S. Miller,³³ C. Mills,⁹ R. Miquel,²⁸ S. Miscetti,¹⁷ G. Mitselmakher,¹⁶ A. Miyamoto,²⁶ Y. Miyazaki,⁴⁰ N. Moggi,⁴ B. Mohr,⁷ R. Moore,¹⁵ M. Morello,⁴⁴ P. A. Movilla Fernandez,²⁸

A. Mukherjee,¹⁵ M. Mulhearn,³¹ T. Muller,²⁵ R. Mumford,²⁴ A. Munar,⁴³ P. Murat,¹⁵ J. Nachtman,¹⁵ S. Nahn,⁵⁹ I. Nakamura,⁴³ I. Nakano,³⁹ A. Napier,⁵⁵ R. Napor,²⁴ D. Naumov,³⁶ V. Necula,¹⁶ F. Niell,³³ J. Nielsen,²⁸ C. Nelson,¹⁵ T. Nelson,¹⁵ C. Neu,⁴³ M. S. Neubauer,⁸ C. Newman-Holmes,¹⁵ T. Nigmanov,⁴⁵ L. Nodulman,² O. Norniella,³ K. Oesterberg,²¹ T. Ogawa,⁵⁶ S. H. Oh,¹⁴ Y. D. Oh,²⁷ T. Ohsugi,²² T. Okusawa,⁴⁰ R. Oldeman,⁴⁹ R. Orava,²¹ W. Orejudos,²⁸ C. Pagliarone,⁴⁴ E. Palencia,¹⁰ R. Paoletti,⁴⁴ V. Papadimitriou,¹⁵ S. Pashapour,³² J. Patrick,¹⁵ G. Pauletta,⁵³ M. Paulini,¹¹ T. Pauly,⁴¹ C. Paus,³¹ D. Pellett,⁶ A. Penzo,⁵³ T. J. Phillips,¹⁴ G. Piacentino,⁴⁴ J. Piedra,¹⁰ K. T. Pitts,²³ C. Plager,⁷ A. Pompos,⁴⁶ L. Pondrom,⁵⁸ G. Pope,⁴⁵ X. Portell,³ O. Poukhov,¹³ F. Prakoshyn,¹³ T. Pratt,²⁹ A. Pronko,¹⁶ J. Proudfoot,² F. Ptohos,¹⁷ G. Punzi,⁴⁴ J. Rademacker,⁴¹ M. A. Rahaman,⁴⁵ A. Rakitine,³¹ S. Rappoccio,²⁰ F. Ratnikov,⁵⁰ H. Ray,³³ B. Reisert,¹⁵ V. Rekovic,³⁶ P. Renton,⁴¹ M. Rescigno,⁴⁹ F. Rimondi,⁴ K. Rinnert,²⁵ L. Ristori,⁴⁴ W. J. Robertson,¹⁴ A. Robson,¹⁹ T. Rodrigo,¹⁰ S. Rolli,⁵⁵ L. Rosenson,³¹ R. Roser,¹⁵ R. Rossin,⁴² C. Rott,⁴⁶ J. Russ,¹¹ V. Rusu,¹² A. Ruiz,¹⁰ D. Ryan,⁵⁵ H. Saarikko,²¹ S. Sabik,³² A. Safonov,⁶ R. St. Denis,¹⁹ W. K. Sakumoto,⁴⁷ G. Salamanna,⁴⁹ D. Saltzberg,⁷ C. Sanchez,³ A. Sansoni,¹⁷ L. Santi,⁵³ S. Sarkar,⁴⁹ K. Sato,⁵⁴ P. Savard,³² A. Savoy-Navarro,¹⁵ P. Schlabach,¹⁵ E. E. Schmidt,¹⁵ M. P. Schmidt,⁵⁹ M. Schmitt,³⁷ L. Scodellaro,¹⁰ A. L. Scott,⁹ A. Scribano,⁴⁴ F. Scuri,⁴⁴ A. Sedov,⁴⁶ S. Seidel,³⁶ Y. Seiya,⁴⁰ F. Semeria,⁴ L. Sexton-Kennedy,¹⁵ I. Sfiligoi,¹⁷ M. D. Shapiro,²⁸ T. Shears,²⁹ P. F. Shepard,⁴⁵ D. Sherman,²⁰ M. Shimojima,⁵⁴ M. Shochet,¹² Y. Shon,⁵⁸ I. Shreyber,³⁵ A. Sidoti,⁴⁴ J. Siegrist,²⁸ M. Siket,¹ A. Sill,⁵² P. Sinervo,³² A. Sisakyan,¹³ A. Skiba,²⁵ A. J. Slaughter,¹⁵ K. Sliwa,⁵⁵ D. Smirnov,³⁶ J. R. Smith,⁶ F. D. Snider,¹⁵ R. Snihur,³² A. Soha,⁶ S. V. Somalwar,⁵⁰ J. Spalding,¹⁵ M. Spezziga,⁵² L. Spiegel,¹⁵ F. Spinella,⁴⁴ M. Spiropulu,⁹ P. Squillacioti,⁴⁴ H. Stadie,²⁵ B. Stelzer,³² O. Stelzer-Chilton,³² J. Strologas,³⁶ D. Stuart,⁹ A. Sukhanov,¹⁶ K. Sumorok,³¹ H. Sun,⁵⁵ T. Suzuki,⁵⁴ A. Taffard,²³ R. Tafirout,³² S. F. Takach,⁵⁷ H. Takano,⁵⁴ R. Takashima,²² Y. Takeuchi,⁵⁴ K. Takikawa,⁵⁴ M. Tanaka,² R. Tanaka,³⁹ N. Tanimoto,³⁹ S. Tapprogge,²¹ M. Tecchio,³³ P. K. Teng,¹ K. Terashi,⁴⁸ R. J. Tesarek,¹⁵ S. Tether,³¹ J. Thom,¹⁵ A. S. Thompson,¹⁹ E. Thomson,⁴³ P. Tipton,⁴⁷ V. Tiwari,¹¹ S. Tkaczyk,¹⁵ D. Toback,⁵¹ K. Tollefson,³⁴ T. Tomura,⁵⁴ D. Tonelli,⁴⁴ M. Tönnemann,³⁴ S. Torre,⁴⁴ D. Torretta,¹⁵ S. Tourneur,¹⁵ W. Trischuk,³² J. Tseng,⁴¹ R. Tsuchiya,⁵⁶ S. Tsuno,³⁹ D. Tsybychev,¹⁶ N. Turini,⁴⁴ M. Turner,²⁹ F. Ukegawa,⁵⁴ T. Unverhau,¹⁹ S. Uozumi,⁵⁴ D. Usynin,⁴³ L. Vacavant,²⁸ A. Vaiciulis,⁴⁷ A. Varganov,³³ E. Vataga,⁴⁴ S. Vajcic III,¹⁵ G. Velev,¹⁵ V. Veszpremi,⁴⁶ G. Veramendi,²³ T. Vickey,²³ R. Vidal,¹⁵ I. Vila,¹⁰ R. Vilar,¹⁰ I. Vollrath,³² I. Volobouev,²⁸ M. von der Mey,⁷ P. Wagner,⁵¹ R. G. Wagner,² R. L. Wagner,¹⁵ W. Wagner,²⁵ R. Wallny,⁷ T. Walter,²⁵ T. Yamashita,³⁹ K. Yamamoto,⁴⁰ Z. Wan,⁵⁰ M. J. Wang,¹ S. M. Wang,¹⁶ A. Warburton,³² B. Ward,¹⁹ S. Waschke,¹⁹ D. Waters,³⁰ T. Watts,⁵⁰ M. Weber,²⁸ W. C. Wester III,¹⁵ B. Whitehouse,⁵⁵ A. B. Wicklund,² E. Wicklund,¹⁵ H. H. Williams,⁴³ P. Wilson,¹⁵ B. L. Winer,³⁸ P. Wittich,⁴³ S. Wolbers,¹⁵ C. Wolfe,¹² M. Wolter,⁵⁵ M. Worcester,⁷ S. Worm,⁵⁰ T. Wright,³³ X. Wu,¹⁸ F. Würthwein,⁸ A. Wyatt,³⁰ A. Yagil,¹⁵ C. Yang,⁵⁹ U. K. Yang,¹² W. Yao,²⁸ G. P. Yeh,¹⁵ K. Yi,²⁴ J. Yoh,¹⁵ P. Yoon,⁴⁷ K. Yorita,⁵⁶ T. Yoshida,⁴⁰ I. Yu,²⁷ S. Yu,⁴³ Z. Yu,⁵⁹ J. C. Yun,¹⁵ L. Zanello,⁴⁹ A. Zanetti,⁵³ I. Zaw,²⁰ F. Zetti,⁴⁴ J. Zhou,⁵⁰ A. Zsenei,¹⁸ and S. Zucchelli⁴

(CDF Collaboration)

¹*Institute of Physics, Academia Sinica, Taipei, Taiwan 11529, Republic of China*²*Argonne National Laboratory, Argonne, Illinois 60439, USA*³*Institut de Física d'Altes Energies, Universitat Autònoma de Barcelona, E-08193, Bellaterra (Barcelona), Spain*⁴*Istituto Nazionale di Fisica Nucleare, University of Bologna, I-40127 Bologna, Italy*⁵*Brandeis University, Waltham, Massachusetts 02254, USA*⁶*University of California at Davis, Davis, California 95616, USA*⁷*University of California at Los Angeles, Los Angeles, California 90024, USA*⁸*University of California at San Diego, La Jolla, California 92093, USA*⁹*University of California at Santa Barbara, Santa Barbara, California 93106, USA*¹⁰*Instituto de Física de Cantabria, CSIC-University of Cantabria, 39005 Santander, Spain*¹¹*Carnegie Mellon University, Pittsburgh, Pennsylvania 15213, USA*¹²*Enrico Fermi Institute, University of Chicago, Chicago, Illinois 60637, USA*¹³*Joint Institute for Nuclear Research, RU-141980 Dubna, Russia*¹⁴*Duke University, Durham, North Carolina 27708, USA*¹⁵*Fermi National Accelerator Laboratory, Batavia, Illinois 60510, USA*¹⁶*University of Florida, Gainesville, Florida 32611, USA*¹⁷*Laboratori Nazionali di Frascati, Istituto Nazionale di Fisica Nucleare, I-00044 Frascati, Italy*¹⁸*University of Geneva, CH-1211 Geneva 4, Switzerland*¹⁹*Glasgow University, Glasgow G12 8QQ, United Kingdom*

- ²⁰Harvard University, Cambridge, Massachusetts 02138, USA
- ²¹The Helsinki Group: Helsinki Institute of Physics, and Division of High Energy Physics, Department of Physical Sciences, University of Helsinki, FIN-00044, Helsinki, Finland
- ²²Hiroshima University, Higashi-Hiroshima 724, Japan
- ²³University of Illinois, Urbana, Illinois 61801, USA
- ²⁴The Johns Hopkins University, Baltimore, Maryland 21218, USA
- ²⁵Institut für Experimentelle Kernphysik, Universität Karlsruhe, 76128 Karlsruhe, Germany
- ²⁶High Energy Accelerator Research Organization (KEK), Tsukuba, Ibaraki 305, Japan
- ²⁷Center for High Energy Physics: Kyungpook National University, Taegu 702-701, Korea; Seoul National University, Seoul 151-742, Korea; and SungKyunKwan University, Suwon 440-746, Korea
- ²⁸Ernest Orlando Lawrence Berkeley National Laboratory, Berkeley, California 94720, USA
- ²⁹University of Liverpool, Liverpool L69 7ZE, United Kingdom
- ³⁰University College London, London WC1E 6BT, United Kingdom
- ³¹Massachusetts Institute of Technology, Cambridge, Massachusetts 02139, USA
- ³²Institute of Particle Physics: McGill University, Montréal, Canada H3A 2T8, and University of Toronto, Toronto, Canada M5S 1A7
- ³³University of Michigan, Ann Arbor, Michigan 48109, USA
- ³⁴Michigan State University, East Lansing, Michigan 48824, USA
- ³⁵Institution for Theoretical and Experimental Physics, ITEP, Moscow 117259, Russia
- ³⁶University of New Mexico, Albuquerque, New Mexico 87131, USA
- ³⁷Northwestern University, Evanston, Illinois 60208, USA
- ³⁸The Ohio State University, Columbus, Ohio 43210, USA
- ³⁹Okayama University, Okayama 700-8530, Japan
- ⁴⁰Osaka City University, Osaka 588, Japan
- ⁴¹University of Oxford, Oxford OX1 3RH, United Kingdom
- ⁴²University of Padova, Istituto Nazionale di Fisica Nucleare, Sezione di Padova-Trento, I-35131 Padova, Italy
- ⁴³University of Pennsylvania, Philadelphia, Pennsylvania 19104, USA
- ⁴⁴Istituto Nazionale di Fisica Nucleare, University and Scuola Normale Superiore of Pisa, I-56100 Pisa, Italy
- ⁴⁵University of Pittsburgh, Pittsburgh, Pennsylvania 15260, USA
- ⁴⁶Purdue University, West Lafayette, Indiana 47907, USA
- ⁴⁷University of Rochester, Rochester, New York 14627, USA
- ⁴⁸The Rockefeller University, New York, New York 10021, USA
- ⁴⁹Istituto Nazionale di Fisica Nucleare, Sezione di Roma 1, University of Roma "La Sapienza," I-00185 Roma, Italy
- ⁵⁰Rutgers University, Piscataway, New Jersey 08855, USA
- ⁵¹Texas A&M University, College Station, Texas 77843, USA
- ⁵²Texas Tech University, Lubbock, Texas 79409, USA
- ⁵³Istituto Nazionale di Fisica Nucleare, University of Trieste/Udine, Italy
- ⁵⁴University of Tsukuba, Tsukuba, Ibaraki 305, Japan
- ⁵⁵Tufts University, Medford, Massachusetts 02155, USA
- ⁵⁶Waseda University, Tokyo 169, Japan
- ⁵⁷Wayne State University, Detroit, Michigan 48201, USA
- ⁵⁸University of Wisconsin, Madison, Wisconsin 53706, USA
- ⁵⁹Yale University, New Haven, Connecticut 06520, USA

(Received 21 January 2005; published 2 June 2005)

We present a measurement of the W^+W^- production cross section using 184 pb^{-1} of $p\bar{p}$ collisions at a center-of-mass energy of 1.96 TeV collected with the Collider Detector at Fermilab. Using the dilepton decay channel $W^+W^- \rightarrow \ell^+ \nu \ell^- \bar{\nu}$, where the charged leptons can be either electrons or muons, we find 17 candidate events compared to an expected background of $5.0_{-0.8}^{+2.2}$ events. The resulting W^+W^- production cross-section measurement of $\sigma(p\bar{p} \rightarrow W^+W^-) = 14.6_{-5.1}^{+5.8}(\text{stat})_{-3.0}^{+1.8}(\text{syst}) \pm 0.9(\text{lum}) \text{ pb}$ agrees well with the standard model expectation.

DOI: 10.1103/PhysRevLett.94.211801

PACS numbers: 13.38.Be, 14.70.Fm

The measurement of the W pair production cross section in $p\bar{p}$ collisions at $\sqrt{s} = 1.96 \text{ TeV}$ provides an important test of the standard model. Anomalous $WW\gamma$ and WWZ triple gauge boson couplings [1], as well as the decays of new particles such as Higgs bosons [2], could result in a rate of W pair production that is larger than the standard

model cross section of $12.4 \pm 0.8 \text{ pb}$ [3]. The first evidence for W pair production was found in $p\bar{p}$ collisions by the Collider Detector at Fermilab (CDF) Collaboration at $\sqrt{s} = 1.8 \text{ TeV}$ [4]. The properties of W pair production have been extensively studied by the CERN LEP Collaborations in e^+e^- collisions up to $\sqrt{s} = 209 \text{ GeV}$

[5], and have been shown to be in good agreement with the standard model. The D0 experiment has recently reported a measurement of the W pair production cross section at Run II of the Fermilab Tevatron [6].

In this Letter we describe a measurement of the W^+W^- production cross section in the dilepton decay channel $W^+W^- \rightarrow \ell^+\nu\ell^-\bar{\nu}$ ($\ell = e, \mu$), and compare the event kinematics with standard model predictions. The signature for $W^+W^- \rightarrow \ell^+\nu\ell^-\bar{\nu}$ events is two high- P_T leptons and missing transverse energy, \cancel{E}_T , from the undetected neutrinos [7]. Jets from the hadronization of additional partons in the event due to initial-state radiation may be present. This analysis is based on $184 \pm 11 \text{ pb}^{-1}$ of data collected by the upgraded CDF during the Tevatron Run II period. For details of the 6% luminosity uncertainty see [8].

The CDF II detector [9] has undergone a major upgrade since the Run I data-taking period. The Central Outer Tracker (COT) is a large-radius cylindrical drift chamber with 96 measurement layers organized into alternating axial and $\pm 2^\circ$ stereo superlayers [10], and is used to reconstruct the trajectories (tracks) of charged particles and measure their momenta. The COT coverage extends to $|\eta| = 1$. A silicon microstrip detector [11,12] provides precise tracking information near the beam line in the region $|\eta| < 2$. The entire tracking volume sits inside a 1.4 T magnetic field. Segmented calorimeters, covering the pseudorapidity region $|\eta| < 3.6$, surround the tracking system. The central ($|\eta| < 1$) and forward ($|\eta| > 1$) electromagnetic calorimeters are lead-scintillator sampling devices, instrumented with proportional and scintillating strip detectors that measure the position and transverse profile of electromagnetic showers. The hadron calorimeters are iron-scintillator sampling detectors. Four layers of planar drift chambers located outside the central hadron calorimeters (CMU) and another set behind a 60 cm thick iron shield (CMP) detect muons with $|\eta| < 0.6$. Additional drift chambers and scintillation counters (CMX) detect muons in the region $0.6 < |\eta| < 1.0$. Gas Cherenkov counters [13] measure the average number of inelastic $p\bar{p}$ collisions per bunch crossing and thereby determine the beam luminosity.

A trigger selects events with a central electron with $E_T > 18 \text{ GeV}$, a muon with $P_T > 18 \text{ GeV}/c$, or a forward electron with $E_T > 20 \text{ GeV}$. For forward electrons, $\cancel{E}_T > 15 \text{ GeV}$ is also required.

Off-line, electron candidates are selected in the central region by matching a well-measured track reconstructed in the fiducial region of the COT to an energy cluster with $E_T > 20 \text{ GeV}$ deposited in the surrounding calorimeters with identification requirements described in detail in [8]. For forward electrons ($1.2 < |\eta| < 2.0$), the track-energy cluster association utilizes a calorimeter seeded silicon tracking algorithm [14].

Muon candidates are selected off-line by demanding $P_T > 20 \text{ GeV}/c$, energy deposition in the calorimeter con-

sistent with that of a minimum ionizing particle, and the same requirements on the reconstructed track as for central electrons. A tightly selected muon category requires the COT track to extrapolate to track segments in either the CMU and CMP chambers or the CMX chambers; a loosely selected category requires the COT track to extrapolate to gaps in the muon chamber coverage.

Significant backgrounds to W^+W^- production in the dilepton decay channel include Drell-Yan events with large \cancel{E}_T (mismeasured in the case of $Z/\gamma^* \rightarrow e^+e^-, \mu^+\mu^-$ or due to ν 's in the case of $Z/\gamma^* \rightarrow \tau^+\tau^-$), W + jet/ γ events in which the jet or photon fakes a lepton, $t\bar{t}$ production, and heavy diboson (WZ, ZZ) production.

All lepton candidates are required to be isolated in order to suppress the background from fake leptons. To be isolated, the fraction of the additional E_T found in a cone with radius $\Delta R = \sqrt{\Delta\phi^2 + \Delta\eta^2} = 0.4$ around the electron (muon) must be less than 10% of the electron E_T (muon P_T). The corresponding isolation requirement calculated using track momenta is also imposed.

Candidate events are required to have two well identified, oppositely charged leptons (electrons or muons), and are classified as $ee, \mu\mu,$ or $e\mu$. An event can contain at most one loose muon. We reject events containing more than two leptons passing all the above identification and isolation criteria. We require events to contain no cone radius 0.4 jets with $E_T > 15 \text{ GeV}$ and $|\eta| < 2.5$.

We require all candidate events to have $\cancel{E}_T > 25 \text{ GeV}$, after the \cancel{E}_T has been corrected for the escaping muon momentum when muon candidates are present. To reduce the likelihood of falsely reconstructed \cancel{E}_T due to mismeasured leptons, the \cancel{E}_T direction must have an azimuthal angle of at least 20° from the closest lepton if the \cancel{E}_T is less than 50 GeV. To further reduce the Drell-Yan background, ee and $\mu\mu$ candidates with a dilepton invariant mass in the Z mass region $76 < M_{\ell\ell} < 106 \text{ GeV}/c^2$ must pass an additional requirement of $\cancel{E}_T^{\text{sig}} > 3 \text{ GeV}^{1/2}$. Here, missing transverse energy significance is defined as $\cancel{E}_T^{\text{sig}} = \cancel{E}_T / \sqrt{\Sigma E_T}$ where ΣE_T is the scalar transverse energy sum over all calorimeter towers. ΣE_T is corrected for muons in an identical manner to the \cancel{E}_T calculation.

The signal acceptance is computed using a large sample of $W^+W^- \rightarrow \ell^+\nu\ell^-\bar{\nu}$ events generated using the PYTHIA Monte Carlo program [15] and passed through a detailed detector simulation. $W \rightarrow \tau\nu$ decays are included, and their contribution to the total acceptance is taken into account. CTEQ5 parton distribution functions (PDF's) [16] are used for the signal as well as the background Monte Carlo samples. The trigger and lepton identification efficiencies are measured using $Z \rightarrow \ell^+\ell^-$ data [8]. The final acceptance estimate for W^+W^- events, assuming a branching ratio $\text{BR}(W \rightarrow \ell\nu) = 0.1068 \pm 0.0012$ [17], is $0.45 \pm 0.05\%$. The number of W^+W^- events expected in the dilepton decay channels is calculated using this accep-

tance number and a NLO (next-to-leading-order) estimate for the total W^+W^- cross section in $p\bar{p}$ collisions at 1.96 TeV of 12.4 ± 0.8 pb [3], using CTEQ6 PDF's [18].

The fraction of W^+W^- events containing no reconstructed jets (“zero-jet fraction”) is calculated using the W^+W^- PYTHIA Monte Carlo sample and multiplied by the ratio of zero-jet fractions measured in Drell-Yan data and PYTHIA Drell-Yan Monte Carlo samples. This scale factor, 0.96 ± 0.06 , corrects for the underestimate of the rate of associated jet production by a leading-order matrix element Monte Carlo program such as PYTHIA. The corrected zero-jet fraction for W^+W^- events is $76 \pm 5\%$.

The systematic uncertainty on the total acceptance for W^+W^- events in the dilepton channel is a combination of uncertainties on the zero-jet fraction (6%), choice of generator and parton shower model (4%), jet energy scale (3%), lepton identification (2%), trigger efficiencies (1%), modeling of the track isolation (4%) and $\cancel{E}_T^{\text{sig}}$ distributions (2%), and choice of PDF (1%). We assume no correlations between these sources of uncertainty and combine them to give an overall 10% systematic uncertainty on the W^+W^- acceptance.

The Drell-Yan background ($Z/\gamma^* \rightarrow e^+e^-, \mu^+\mu^-, \tau^+\tau^-$) is estimated using a combination of data and Monte Carlo samples, including a large sample of PYTHIA generated Drell-Yan events. The Drell-Yan background estimate in the $e\mu$ channel is entirely Monte Carlo calculation based. The background from $Z/\gamma^* \rightarrow \tau^+\tau^-$ in all detection channels is also based on Monte Carlo calculations alone. In the like-flavor dilepton channels ee ($\mu\mu$), the background from $Z/\gamma^* \rightarrow e^+e^-$ ($Z/\gamma^* \rightarrow \mu^+\mu^-$) is estimated with a method described next that makes use of both Monte Carlo calculations and data. The background estimate outside the Z mass window starts by counting the number of data events inside the Z mass window that pass all the W^+W^- selection criteria applied outside. This number of events is multiplied by the ratio of the number of Drell-Yan events outside and inside the Z mass window, estimated using Monte Carlo simulations after all out-of-window selection criteria have been applied. The same method is applied to estimate the background inside the Z mass window, using the ratio of events that pass both \cancel{E}_T and $\cancel{E}_T^{\text{sig}}$ cuts to those that fail one or both of these requirements. Monte Carlo is needed to estimate a significant contamination from non-Drell-Yan events in the data samples used in this procedure. W^+W^- events themselves contribute to this contamination. This dependence of the Drell-Yan background estimate on the W^+W^- cross section, and vice versa, is resolved by iteratively finding a common solution to both. Statistical uncertainties on the data dominate the final systematic uncertainty on the Drell-Yan background.

We estimate the fake lepton background contribution by applying a P_T dependent lepton fake rate to $\ell + \cancel{E} + d$ events, where d denotes any object which could fake a

lepton. Such events must pass all other W^+W^- selection criteria. The lepton fake rates are defined by the ratio N_ℓ/N_d . Objects that can fake leptons that are counted in the denominator (N_d) are jets with $E_T > 20$ GeV and $|\eta| < 2$ for electrons and tracks with $P_T > 20$ GeV/ c and $E/P < 1$ for muons. The numerator (N_ℓ) is the number of objects passing all lepton identification and isolation criteria. The lepton fake rates are determined using large samples of jet triggered data with jet E_T thresholds in the range 20–100 GeV, correcting for the presence of real leptons from W and Z production. The probability for an object to fake a lepton is of the order 10^{-4} to 10^{-3} depending on the lepton type and detector region. Studies of fake rate variations between jet samples with different trigger thresholds and using various object definitions of objects that can fake leptons have been performed. The estimated systematic uncertainty on this background is 40%.

The $W\gamma$ background estimate is derived using a leading-order Monte Carlo generator for the process $p\bar{p} \rightarrow W\gamma X \rightarrow \ell\nu\gamma X$ [19], which has been interfaced to PYTHIA for the purposes of parton showering and hadronization. The sample is normalized to a NLO calculation of the $W\gamma$ cross section [20]. The $W\gamma$ background that is double counted in the fake lepton background estimate described above is determined to be negligible.

The remaining backgrounds from $t\bar{t}$, WZ , and ZZ production are calculated using Monte Carlo samples generated with PYTHIA and normalized to NLO cross sections. The background from top pair production in the dilepton decay channel ($t\bar{t} \rightarrow W^+bW^- \bar{b} \rightarrow \ell^+ \nu b \ell^- \bar{\nu} \bar{b}$) is greatly reduced by the zero-jet requirement. The background from WZ production has two main contributions: $WZ \rightarrow q\bar{q}'\ell^+\ell^-$, which is largely rejected by the zero-jet requirement, and $WZ \rightarrow \ell\nu\ell^+\ell^-$, which is largely rejected by the veto on trilepton events. The background coming from ZZ production is predominantly due to $ZZ \rightarrow \ell^+\ell^-\nu\bar{\nu}$. The final systematic uncertainty on the total background estimate is approximately 45%, dominated by the uncertainty on the Drell-Yan background.

The signal and background expectations are summarized in Table I, together with the number of data events passing the selection criteria [21]. The measured cross section is

$$\sigma(W^+W^-) = 14.6^{+5.8}_{-5.1}(\text{stat})^{+1.8}_{-3.0}(\text{syst}) \pm 0.9(\text{lum}) \text{ pb},$$

where the systematic uncertainty is a combination of the uncertainties on the signal acceptance and background estimates. The third uncertainty corresponds to a 6% uncertainty from the integrated luminosity measurement. The dilepton mass and lepton transverse momenta distributions are shown in Fig. 1. There is no evidence for statistically significant discrepancies in either the dilepton mass or lepton transverse momentum distributions, which could indicate the presence of poorly estimated backgrounds or physics beyond the standard model.

TABLE I. Estimated backgrounds, W^+W^- signal, and the observed number of events in 184 pb^{-1} for each dilepton category. The W^+W^- expectation assumes a total cross section of 12.4 pb . Systematic uncertainties are included.

	ee	$\mu\mu$	$e\mu$
$Z/\gamma^* \rightarrow \ell^+\ell^-$	$0.21_{-0.16}^{+1.29}$	$0.43_{-0.38}^{+1.56}$	0.43 ± 0.14
WZ	0.29 ± 0.03	0.33 ± 0.03	0.15 ± 0.02
ZZ	0.35 ± 0.04	0.34 ± 0.04	0.011 ± 0.002
$W + \gamma$	0.48 ± 0.13	—	0.57 ± 0.13
$t\bar{t}$	0.021 ± 0.011	0.012 ± 0.007	0.046 ± 0.018
Fake	0.52 ± 0.19	0.17 ± 0.16	0.65 ± 0.37
Background	$1.9_{-0.3}^{+1.3}$	$1.3_{-0.4}^{+1.6}$	1.9 ± 0.4
Expected WW	2.6 ± 0.3	2.5 ± 0.3	5.1 ± 0.6
Total expected	$4.5_{-0.5}^{+1.4}$	$3.8_{-0.5}^{+1.6}$	7.0 ± 0.8
Observed	6	6	5

We have performed an alternative measurement of the W^+W^- production cross section, which tests the robustness of our result in a sample with different signal and background composition. The event selection is based on the “lepton + track” analysis used for our measurement of the $t\bar{t}$ production cross section in the dilepton channel [22].

There are two important differences between the lepton + track analysis and our main analysis. First, one of the two lepton candidates is required only to be an isolated track. Second, all events must pass a $\cancel{E}_T^{\text{sig}}$ requirement of $\cancel{E}_T^{\text{sig}} > 5.5 \text{ GeV}^{1/2}$ where, here, the E_T sum is made over all jets with $E_T > 5 \text{ GeV}$. The candidate isolated track must have $P_T > 20 \text{ GeV}/c$ and be in the range $|\eta| < 1$. Again, only events with no jets are considered. The overall acceptance is $0.42\% \pm 0.05\%$, similar to the acceptance for the main analysis. The increased acceptance for dilepton events where electrons or muons pass through gaps in the calorimetry or muon system and for single prong hadronic decays of the τ lepton from $W \rightarrow \tau\nu$ is offset by the more restrictive $\cancel{E}_T^{\text{sig}}$ cut required to control the larger backgrounds.

The numbers of observed events, the expected standard model backgrounds, and the predicted W^+W^- signal are compared for both analyses in Table II. The higher background rates for the lepton + track analysis are mainly due to the fake lepton background contribution coming from the isolated track. The resulting cross-section measurement using the lepton + track selection is

$$\sigma(W^+W^-) = 24.2 \pm 6.9(\text{stat})_{-3.7}^{+5.2}(\text{syst}) \pm 1.5(\text{lum}) \text{ pb}.$$

The two measurements are statistically compatible with one another given an estimated 43% overlap in signal acceptance. Since combining the results of these two analyses does not result in a significant reduction of the uncertainty, we quote as the final result of this measure-

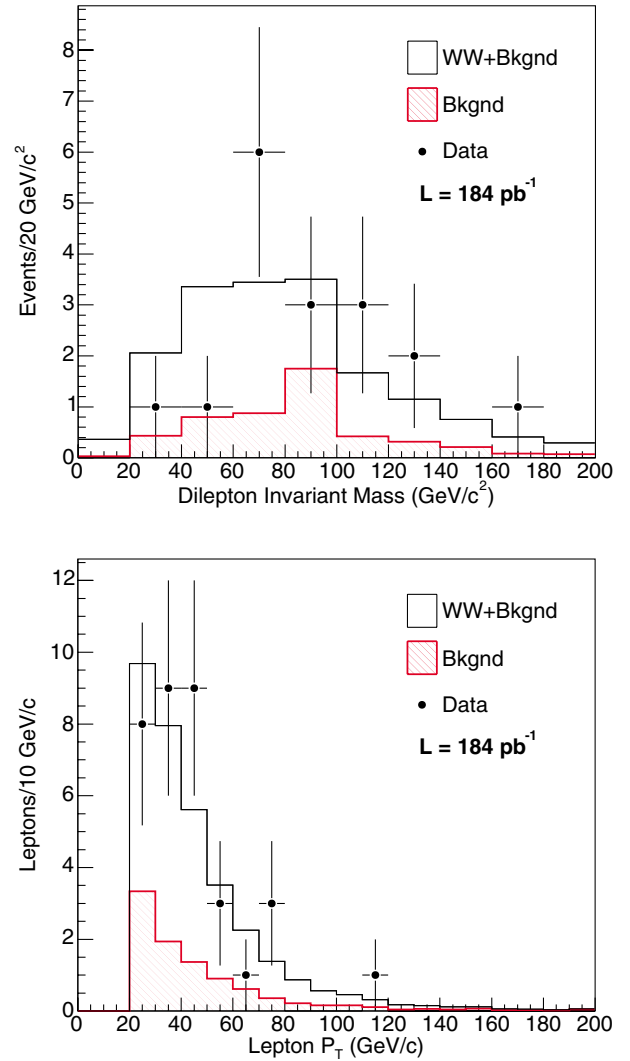


FIG. 1 (color online). The dilepton mass (top) and lepton transverse momentum distribution (bottom) for the candidate events in comparison with the standard model expectation. Kolmogorov-Smirnov tests of these distributions yield p values of 13% (top) and 78% (bottom).

ment the analysis with the best *a priori* sensitivity, which is the analysis summarized in Table I.

In summary, we have measured the W^+W^- cross section in $p\bar{p}$ collisions at $\sqrt{s} = 1.96 \text{ TeV}$ to be $14.6_{-6.0}^{+6.1} \text{ pb}$. This is based on the observation of 17 events consistent with originating from W pair production and subsequent decay to two charged leptons, compared to a total estimated background of $5.0_{-0.8}^{+2.2}$ events. The measured cross section is consistent with a NLO standard model prediction and is corroborated by an independent lepton + track analysis.

We thank the Fermilab staff and the technical staffs of the participating institutions for their vital contributions. We also thank John Campbell and Keith Ellis for many useful discussions. This work was supported by the U.S. Department of Energy and National Science Foundation;

TABLE II. Estimated backgrounds, W^+W^- signal, and the observed number of events for both the main (MAIN) analysis using 184 pb^{-1} and the lepton + track (LTRK) analysis using 197 pb^{-1} . The signal expectation assumes a total W^+W^- cross section of 12.4 pb . Systematic uncertainties are included.

	MAIN	LTRK
Drell-Yan ($Z/\gamma^* \rightarrow \ell^+\ell^-$)	$1.06^{+2.03}_{-0.44}$	$1.81^{+2.36}_{-1.38}$
WZ	0.76 ± 0.06	1.01 ± 0.24
ZZ	0.70 ± 0.07	0.76 ± 0.18
$W + \gamma$	1.06 ± 0.19	0.33 ± 0.13
$t\bar{t}$	0.078 ± 0.023	0.18 ± 0.04
Fake	1.34 ± 0.66	7.96 ± 3.47
Background	$5.0^{+2.2}_{-0.8}$	$12.1^{+4.2}_{-3.8}$
Expected WW	10.20 ± 1.19	10.23 ± 1.37
Total expected	$15.2^{+2.5}_{-1.5}$	$23.0^{+4.4}_{-4.0}$
Observed	17	32

the Italian Istituto Nazionale di Fisica Nucleare; the Ministry of Education, Culture, Sports, Science, and Technology of Japan; the Natural Sciences and Engineering Research Council of Canada; the National Science Council of the Republic of China; the Swiss National Science Foundation; the A. P. Sloan Foundation; the Bundesministerium fuer Bildung und Forschung, Germany; the Korean Science and Engineering Foundation and the Korean Research Foundation; the Particle Physics and Astronomy Research Council and the Royal Society, U.K.; the Russian Foundation for Basic Research; the Comisión Interministerial de Ciencia y Tecnología, Spain; and in part by the European Community's Human Potential Programme under Contract No. HPRN-CT-2002-00292, Probe for New Physics.

- [1] J. Ellison *et al.*, *Annu. Rev. Nucl. Part. Sci.* **48**, 33 (1998).
 [2] Benjamin W. Lee, C. Quigg, and H. B. Thacker, *Phys. Rev. D* **16**, 1519 (1977); M. Dittmar and H. Dreiner, *Phys. Rev. D* **55**, 167 (1997).

- [3] J. M. Campbell and R. K. Ellis, *Phys. Rev. D* **60**, 113006 (1999), NLO calculation using MCFM version 3.4.5.
 [4] F. Abe *et al.*, *Phys. Rev. Lett.* **78**, 4536 (1997).
 [5] LEP Collaborations, hep-ex/0312023; R. Barate *et al.* (ALEPH Collaboration), *Phys. Lett. B* **484**, 205 (2000); P. Abreu *et al.* (DELPHI Collaboration), *Phys. Lett. B* **479**, 89 (2000); M. Acciarri *et al.* (L3 Collaboration), *Phys. Lett. B* **496**, 19 (2000); G. Abbiendi *et al.* (OPAL Collaboration), *Phys. Lett. B* **493**, 249 (2000).
 [6] V. M. Abazov *et al.*, hep-ex/0410066 [*Phys. Rev. Lett.* (to be published)].
 [7] We use a coordinate system where θ is the polar angle to the proton beam, ϕ is the azimuthal angle about this beam axis, and η is the pseudorapidity defined as $-\ln(\tan(\theta/2))$. The transverse momentum of a particle is denoted by $P_T \equiv P \sin\theta$. The analogous quantity defined using energies, defined as $E_T \equiv E \sin\theta$, is called transverse energy. Missing transverse energy, \cancel{E}_T , is defined as the magnitude of $-\sum_i E_T^i \hat{n}_i$, where \hat{n}_i is a unit vector in the azimuthal plane that points from the beam line to the i th calorimeter tower.
 [8] D. Acosta *et al.*, *Phys. Rev. Lett.* **94**, 091803 (2005).
 [9] R. Blair *et al.*, FERMILAB-PUB-96-390-E.
 [10] T. Affolder *et al.*, *Nucl. Instrum. Methods Phys. Res., Sect. A* **526**, 249 (2004).
 [11] A. Sill *et al.*, *Nucl. Instrum. Methods Phys. Res., Sect. A* **447**, 1 (2000).
 [12] A. Affolder *et al.*, *Nucl. Instrum. Methods Phys. Res., Sect. A* **453**, 84 (2000).
 [13] D. Acosta *et al.*, *Nucl. Instrum. Methods Phys. Res., Sect. A* **461**, 540 (2001).
 [14] C. Issever, *AIP Conf. Proc.* **670**, 371 (2003).
 [15] T. Sjöstrand *et al.*, *Comput. Phys. Commun.* **135**, 238 (2001).
 [16] H. L. Lai *et al.*, *Eur. Phys. J. C* **12**, 375 (2000).
 [17] K. Hagiwara *et al.* (Particle Data Group), *Phys. Rev. D* **66**, 010001 (2002).
 [18] J. Pumplin *et al.*, *J. High Energy Phys.* 07 (2002) 012.
 [19] U. Baur and E. L. Berger, *Phys. Rev. D* **41**, 1476 (1990).
 [20] D. Acosta *et al.*, *Phys. Rev. Lett.* **94**, 041803 (2005).
 [21] Of the 17 events selected, 2 are also selected by the analysis described in D. Acosta *et al.*, FERMILAB-PUB-05-002-E, hep-ex/0501021 [*Phys. Rev. D* (to be published)].
 [22] D. Acosta *et al.*, *Phys. Rev. Lett.* **93**, 142001 (2004).